Theor Chem Acc (2009) 124:71–83
DOI 10.1007/s00214-009-0582-4

REGULAR ARTICLE

Glutathione transferase A1-1: catalytic role of water

Daniel F. A. R. Dourado · Pedro Alexandrino Fernandes · Maria João Ramos

Received: 3 March 2009 / Accepted: 6 May 2009 / Published online: 2 June 2009

Abstract For more than almost 30 years now, glutathione transferases (GSTs) have been known as xenobiotic/endobiotic detoxification enzymes. GSTs catalyze the nucleophilic addition of glutathione (GSH) sulphur thiolate to a wide range of electrophilic substrates, building up a less toxic and more soluble compound, which can then be removed from the cell. Recently we proposed a consistent GSH activation mechanism. By performing QM/MM calculations, we demonstrated that a water molecule, following a first conformational rearrangement of GSH, is capable of assisting a proton transfer between the GSH thiol and alpha carboxylic groups. In this study we go further in the analysis of the water role in GSH activation by performing a long Molecular Dynamics (MD) study on glutathione transferase A1-1 Thr68 mutants complexed with GSH and the GSH decarboxylated analogue (dGSH), for which experimental kinetic data are available.

Keywords Glutathione transferase · Role of water · Molecular dynamics · GSH activation

1 Introduction

Glutathione transferases (GSTs) are crucial enzymes in the cell detoxification process. They have been described as the most important enzymes involved in the metabolism of electrophilic compounds [1]. This study focuses on glutathione transferase A1-1 (GSTA1-1), the most studied alpha cytosolic GST [2–14]. GSTA1-1 is a homodimer, each subunit having a *G-site* where glutathione (GSH) substrate binds and an *H-site* pocket for electrophilic substrates. When GSH binds to the *G-site*, the p*K*a of its thiol group in GSH drops 1.5 pH units promoting its deprotonation [15]. After GSH activation, the nucleophilic sulphur atom attacks the electrophilic toxic compound (R–X) present in the *H-site*, producing a less dangerous and more soluble compound (GSR).

$$\mathrm{GSH} + \mathrm{R{-}X\,(electrophilic\,substrate)} \rightarrow \mathrm{GSR} + \mathrm{H^+\,X^-}$$

The product (GSR) release, controlled by the C-terminal domain, is a rate-limiting step of catalysis for fast substrates [8].

In terms of structural domains, each subunit is composed of a distinct N-terminal alpha/beta domain, which adopts the thioredoxin fold and a C-terminal all-helical domain [16]. The *G-site*, which is only completed on dimerization, is found in a cleft between the N and C-terminal domains. All the important residues for catalysis are in the N-terminal domain [16].

1.1 GSTA1-1 G-Site

In the *G-Site* of GSTA1-1, three important aminoacids can be identified [17] (Fig. 1).

The first one is Tyr9 which establishes a hydrogen bond with the thiol group of GSH. In some earlier studies it was suggested that Tyr, behaving like a base, would activate GSH by receiving the proton from its thiol group [18].

Electronic supplementary material The online version of this article (doi:10.1007/s00214-009-0582-4) contains supplementary material, which is available to authorized users.

D. F. A. R. Dourado · P. A. Fernandes · M. J. Ramos (✉)
REQUIMTE/Departamento de Química, Faculdade de Ciências, Universidade do Porto, Rua do Campo Alegre, 687, 4169-007 Porto, Portugal
e-mail: mjramos@fc.up.pt

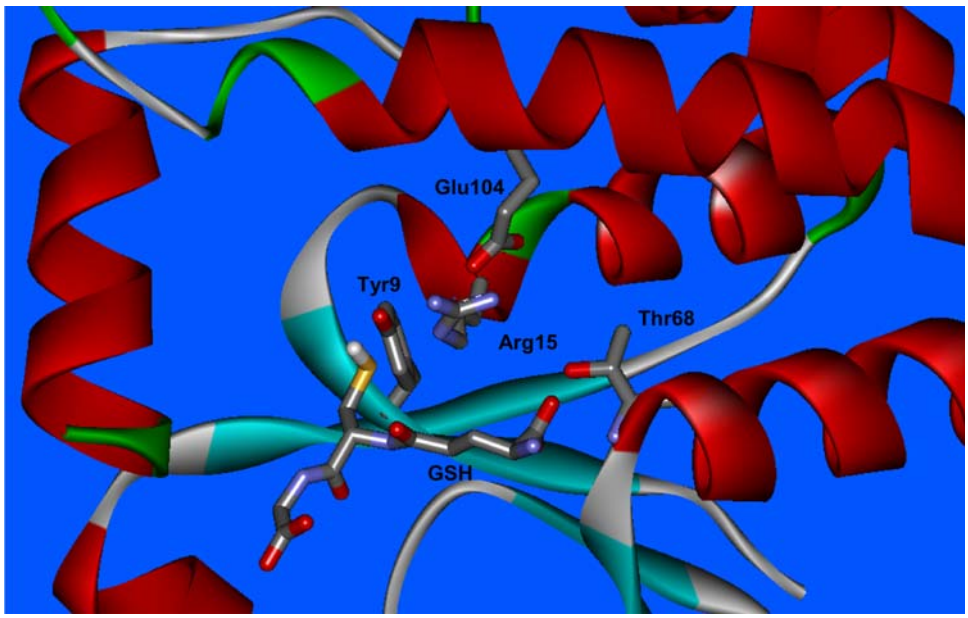

Fig. 1 GSTA1-1 active center *G-site*

As the optimal pH Value for GST activity ($\sim$7.4) is below the last measured tyrosine p*K*a value (8.1), it has been concluded that the tyrosine should be protonated and therefore play the role of hydrogen bond donor rather than that of a base, stabilizing the deprotonated form of glutathione nucleophilic cysteine [12].

The second aminoacid is Arg15, a strictly conserved residue in Alpha glutathione transferases, involved in a salt-bridge with glu104. Mutations in Arg15 led to a great reduction in the catalytic activity of GSTA1-1 [12]. The precise role of Arg15 remains poorly understood.

The third aminoacid is Thr68 which is hydrogen bonded to the glutamyl alpha carboxylate of GSH. The glutamyl alpha carboxylate has been considered essential to catalysis [2, 7, 19–21]. Experimental studies with GSTA1-1 have shown that when a decarboxylated analogue of glutathione (4-aminobutyric acid(GABA)-Cys-Gly, dGSH) is used with the substrate chloro-2,4-dinitrobenzene (CNDB), K_{cat}/K_M drops 15,000 times [2]. The p*K*a of thiol rises to values of a non-enzymatic reaction (6.7–9.2 pH units), and the substrate dGSH has a lower affinity for the *G-site* active center, as K_M^{dGSH} is 100-fold higher than K_M^{GSH} [2].This last fact seems to result from the loss of the two strong hydrogen bonds between the glutamyl alpha carboxylate and Thr68.

The same studies using the glutathione analogue dGSH also concluded that the T68E mutation and to a less extent T68D restored part of the catalytic activity. In fact, for the T68E mutant, a 10-fold increase in the K_{cat} relative to the wild-type GST with dGSH is observed, most probably reflecting a decrease in the p*K*a of dGSH thiol group to 8.2 pH units [2]. It was proposed that the T68E mutation would insert a carboxylic group capable of taking the place of the alpha carboxylic group of GSH glutamate since, in the wild-type enzyme, threonine 68 side chain and backbone establish hydrogen bonds with the alpha carboxylic group of GSH glutamate. In a recently obtained crystallographic structure of GSTA1-1 T68E mutated enzyme complexed with GSH, Glu68 is not facing the substrate [13] and a Cl^- ion is taking the place of the alpha carboxylic group of GSH glutamate. The exact reason why the chlorine ion takes the place of the glutamate is unclear; however, it seems reasonable to think that in physiological conditions, the outcome of the chlorine/carboxylate competition for the binding pocket will be different eventually. When GSH is used instead, substitution of a hydroxyl to a methyl group in the T68V mutation leads to a reduction in the K_{cat} of three- to sixfold and a K_M^{GSH} increase of approximately twofold [7], depending on the electrophile substrate used. For the T68E mutant, due to a change in the rate-limiting step, the K_{cat} is slightly higher than the one of the wild-type enzyme [2]. On the other hand, the increase in the K_M^{GSH} is of $\sim$18-fold, which results in an overall K_{cat}/K_M lower than the one observed for GSTA1-1 [2].

Water molecules also seem to have an important role in catalysis. Based on the crystallographic structures of cytosolic GSTs, it has been suggested that water molecules in the *G-site* could assist the proton release and extrusion [4, 22]. Potentiometric experiments with pi, alpha and mu class enzymes concluded that the proton from the GSH thiol group could be released into the surrounding solution after the formation of the GST–GSH complex in the absence of any enzyme turnover [15, 23]. It was suggested that the process follows a multistep mechanism [15]. First, a precomplex Enzyme—GSH turns into a more stable Enzyme*—GSH Michaelis complex this being the rate-

limiting step; then two fast events occur, GSH ionization followed by proton extrusion.

Recently, we proposed a GSH activation mechanism that is consistent with the known data about the influence of the glutamyl alpha carboxylate and *G-site* water molecules in catalysis [24]. Our studies have shown that after a first conformational rearrangement of GSH ($\Delta G_{conf} = -1.62$ kcal mol^{-1}), a water molecule is able to assist a proton transfer between GSH thiol and alpha carboxylic groups, with an activation energy of 13.39 kcal mol^{-1}. This energy barrier is in agreement with the experimental kinetics for the GST-catalyzed GSH–CNDB conjugation, a common electrophilic substrate ($K_{cat} = 88 \pm 3$ s^{-1}, $\Delta G^{\ddagger} = 15.06$ kcal mol^{-1} [7]). A direct proton transfer between the two GSH active groups has been shown to be very improbable, as the free energy barrier (35.32 kcal mol^{-1}) is too high for a catalyzed reaction and does not match the experimental kinetics.

The goal of this study is to further understand the role of water as well as the GSH thiol and glutamyl alpha carboxylate groups in GSH activation, while elucidating the structural/catalytic reasons behind the experimental results obtained for the Thr68 mutants. In order to achieve that goal, a set of molecular dynamics studies of GSTA1-1 wild type and Thr68 mutant enzymes complexed with GSH and dGSH was performed. For the substrate GSH, we have studied the wild-type enzyme (GSTA1-1) and the mutants, T68E (GSTA1-1_T68E) and T68V (GSTA1-1_T68V). For dGSH, the glutathione-decarboxylated analogue, we have studied the wild-type enzyme (GSTA1-1_dGSH) and the mutants, T68E (GSTA1-1_T68E_dGSH) and T68D (GSTA1-1_T68D_dGSH).

2 Method

The crystallographic structure of GSTA1-1 complexed with GSH was obtained in the Protein Data Bank [25] (pdb code: 1PKW).

The mutated enzymes GSTA1-1_T68E, GSTA1-1_T68D and GSTA1-1_T68V, were built with the SwissPdb Viewer software [26] starting from the GSTA1-1 structure complexed with GSH.

GSTA1-1_dGSH and the mutated enzymes that use dGSH as the substrate, GSTA1-1_T68E_dGSH and GSTA1-1_T68D_dGSH, were built also from the same crystallographic structure but with GSH converted to dGSH, its decarboxylated analogue, using GaussView 3.09 [27]. In order to further elucidate whether Glu68 could replace or assist the glutamyl alpha carboxylic group in GSH activation, we used a different rotamer in each T68E mutant enzyme subunit complexed with the substrates GSH and dGSH. In subunit 1, the Glu68 side chain was turned towards the GSH glutamate carboxylic group (as expected for dGSH), and in subunit 2, it was set in the opposite direction (as seen in GSTA1-1_T68E crystallographic structure with the bond Cl^{-} [13]).

The residue gamma-glutamate of GSH and the molecule GABA (4-aminobutyric acid) of dGSH have to be parameterized, since the AMBER99 force field [28, 29] lacks a full parameterization of these species.

The dihedrals, angles, bonds and vdw parameters were based on the AMBER99 force field. Atomic point charges were calculated with the GAUSSIAN software package following the methodology used in the AMBER99 force field through the fitting of the HF/6-31G* electrostatic potential to atomic point charges using the ESP (RESP) algorithm.

The molecular dynamics simulations and the subsequent analyses were carried out using the Gromacs software package conjugated with the Amber99 force field [28–31].

All the enzymes were solvated with ~17000 single point charge waters (SPC) [32], and then were submitted to 100 steps of steepest descent energy minimization to remove bad contacts between the solvent and the protein. Subsequently, the system was equilibrated for 200 ps, maintaining the protein atoms restrained by weak harmonic constraints to allow for the structural relaxation of the waters. Isothermal–isobaric molecular dynamics (MD) simulations of 3 ns with a time-step of 0.002 ps were performed, and the trajectories were saved at each 1 ps. For the mutant enzyme GSTA1-1_T68E_dGSH, to further support the results found, the initial 3 ns MD simulation was extended to 20 ns.

Periodic boundary conditions were used in all the simulations. The temperature and pressure were maintained constant by the use of the Berendsen temperature coupling and pressure coupling (parameters: $\tau_T = 0.1$ ps, $T_{ref} = 300$ K, $P_{ref} = 1$ bar) [33]. The Particle Mesh Ewald (PME) [34] method was applied to compute electrostatic interactions with a cut-off of 1.0 nm. In terms of van der Walls interactions, a twin range cut-off, with neighbour list cut-off 1.0 and van der Waals cut-off of 1.0, was used. All the bonds involving hydrogen atoms were constrained by the LINCS constraint algorithm [35].

3 Results and discussion

The initial crystallographic structures of all the enzyme homodimers show some structural differences that were accentuated during the MD simulations. The time dependence of the root mean square deviation (RMSD) of the backbone structure with respect to the initial structure ($t = 0$) was analyzed for all the enzyme subunits. The RMSD converged in all of them, attesting that the 3 ns long simulations provided significant sampling.

Radial distribution functions (RDFs) for the thiol and alpha carboxylate groups, relative to the water oxygen atoms (OW), were calculated to follow the water arrangement around GSH while complexed with the enzymes studied. As a reference, the RDFs calculated for GSH free in solution were used. In fact, RDFs, such as the ones calculated here, describe fluctuations in density around a given atom as a function of radial distance. They represent the probability of finding two atoms at a defined distance apart, relative to the probability of a completely random distribution at macroscopic density. An RDF plot shows the average location of the atoms. Normally up to a certain distance (the sum of the atomic radius), the plot value is zero; then, a large peak defining an average distance between the atoms takes place if a significant attractive interaction between them exists.

Average structures of all the enzymes studied were also analyzed to observe any structural divergences in residue 68 mutant enzymes when compared with the wild-type enzyme. All these results will be presented next.

3.1 RDFs for selected solvent: GSH pairs of heavy atoms in aqueous solution

When substrate GSH is free in solution, the thiol group possesses a water coordination sphere composed of nine molecules. The S–OW RDF (OW = water oxygen) peak starts at 0.275 nm, has a maximum at 0.345 nm and becomes zero at 0.485 (Fig. 2a).

Around each of the GSH glutamyl alpha carboxylate group oxygen atoms, two well-defined water coordination spheres are observed (Fig. 2b). The first O–OW RDF peak is very intense and corresponds to three water molecules. It starts at 0.235 nm, has a maximum at 0.265 nm and ends at 0.330 nm. The second peak, on the other hand, starts at 0.330 nm, has a maximum at 0.475 nm and becomes zero at 0.530 nm in a total of 13 water molecules.

3.2 GSTA1-1

Around the GSH thiol group, in both the subunits, a well-defined water coordination sphere composed of six water molecules can be found (Fig. 3). The average RDF for the S–OW pair in subunits 1 and 2 shows a peak that starts at 0.280 nm, reaches a maximum at 0.339 and ends at 0.509 nm. Comparing it with the GSH S–OW peak (Fig. 2a), we can conclude that in the enzyme environment a water organization around the GSH thiol group still exists; however, in this case, it is composed of less waters since the peak is less intense.

On analyzing each one of the glutamyl alpha carboxylate group oxygen atoms separately, (Fig. 4) we can observe that as opposed to what happens to GSH in solution (Fig. 2b), the water is asymmetrically distributed. In fact, a very well-defined water arrangement can be detected for O2 in both the subunits (Fig. 4b). GSH O2–OW RDF plots show an extremely defined peak for the first coordination sphere that corresponds to precisely one water molecule. The peak starts at 0.245 nm, has a maximum at 0.265 nm and goes to zero at 0.335 nm. This water coordination sphere is then followed by two others composed of four and eight molecules, respectively.

If we analyze the *G-site* MD average structure, it is possible to observe that mainly around the GSH thiol group, the subunits evolved differently (Fig. 5). In subunit 2, contrary to what happens in subunit 1, GSH thiol is not hydrogen bonded to Tyr9 since the thiol sulphur is distant from the Tyr oxygen by 0.506 nm. On the other hand, the GSH glutamyl alpha carboxylic and amino group are bound to the *G-site* pocket in a similar manner in both the

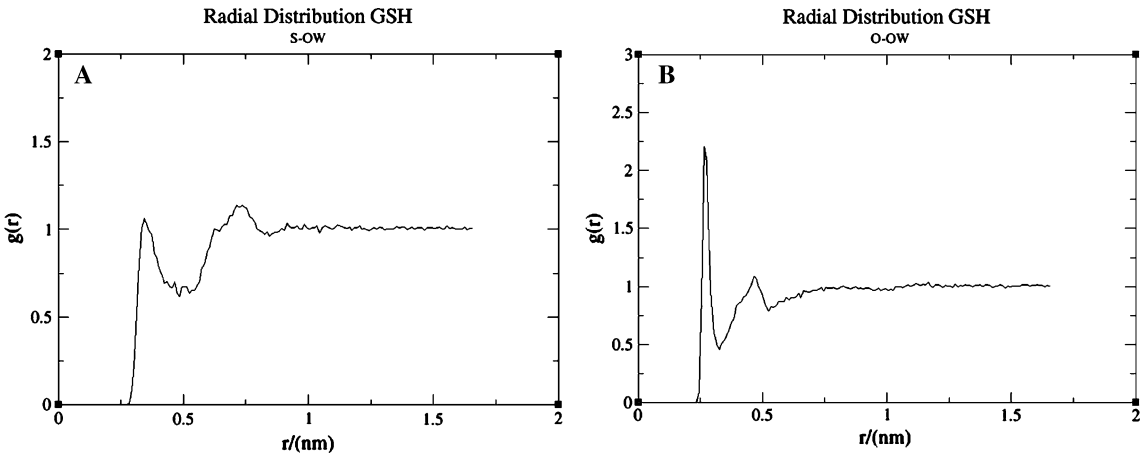

Fig. 2 **a** Substrate GSH S–OW radial distribution function. Coordination sphere—nine water molecules. **b** Average GSH COO oxygen atoms radial distribution function. First coordination sphere—three water molecules and second coordination sphere—13 water molecules

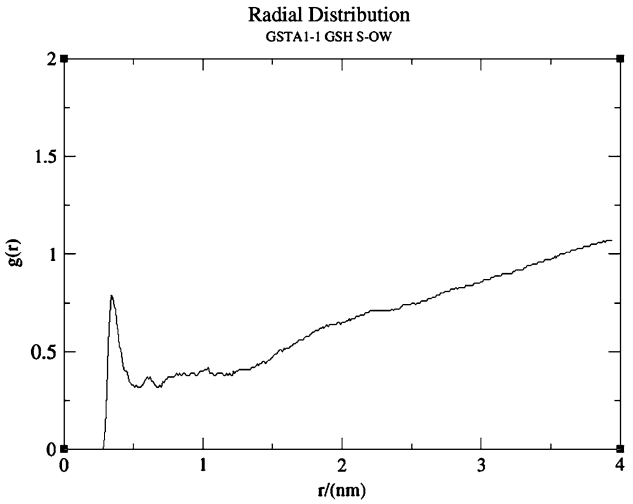

Fig. 3 Subunits 1 and 2 average GSTA1-1 GSH S–OW radial distribution function. Coordination sphere—six water molecules

subunits. One of the carboxylic oxygen atoms is hydrogen bonded to Thr68 mainchain (Fig. 5d), while the other establishes a hydrogen bond with the Thr68 side chain (Fig. 5f). The amino group is hydrogen bonded to the Gln67 side chain (Fig. 5e).

3.3 GSTA1-1 mutants

3.3.1 GSTA1-1_T68V

For GSTA1-1_T68V, a less intense S–OW RDF peak shows that only three water molecules are organized around the thiol group. The peak starts at 0.275 nm, reaches a maximum at 0.345 nm and ends at 0.465 nm. Therefore, in this mutant, a 50% decrease in the water arrangement around the thiol group is observed.

Concerning the GSH glutamyl alpha carboxylate, we can also find some differences in the water arrangement. For subunit 2, the O–OW RDF plots are identical to those observed in the wild-type enzyme (Fig. 4). Therefore, in subunit 2, we can detect an asymmetric water distribution around the two alpha carboxylic group oxygen atoms, with O2 showing a very well-defined peak for the first coordination sphere, which is composed of just 1 water molecule, followed by two other coordination spheres. On the other hand, for GSTA1-1_T68V subunit 1, contrary to what happens for the wild-type enzyme, the RDF plots O1–OW (Fig. 6a) and O2–OW (Fig. 6b) are identical; therefore, the water is identically distributed around the two oxygen atoms.

Comparing the *G-site* MD average structures of both the enzymes, it is possible to make the following considerations. In both the subunits of the GSTA1-1_T68V mutant, the hydrogen bond between the GSH glutamyl alpha carboxylate and the residue 68 side chain is lost (Fig. 7, subunit 1 example). On the other hand, the hydrogen bond between the same GSH glutamyl alpha carboxylate and residue 68 mainchain is maintained (Fig. 7d, subunit 1 example). In subunit 1 of GSTA1-1_T68V, the Gln67 side chain does not have the same rotamer as the wild-type structure; therefore, the hydrogen bond that it establishes with the GSH glutamyl alpha amino group is lost (Fig. 7e). The loss of this interaction seems to dictate the different water arrangement obtained around the glutamyl alpha carboxylate oxygen atoms in this subunit.

In fact, the loss of these fundamental hydrogen bonds between the GSH-pocket and the substrate GSH is reflected in the experimental K_M^{GSH} increase of approximately two-fold [7].

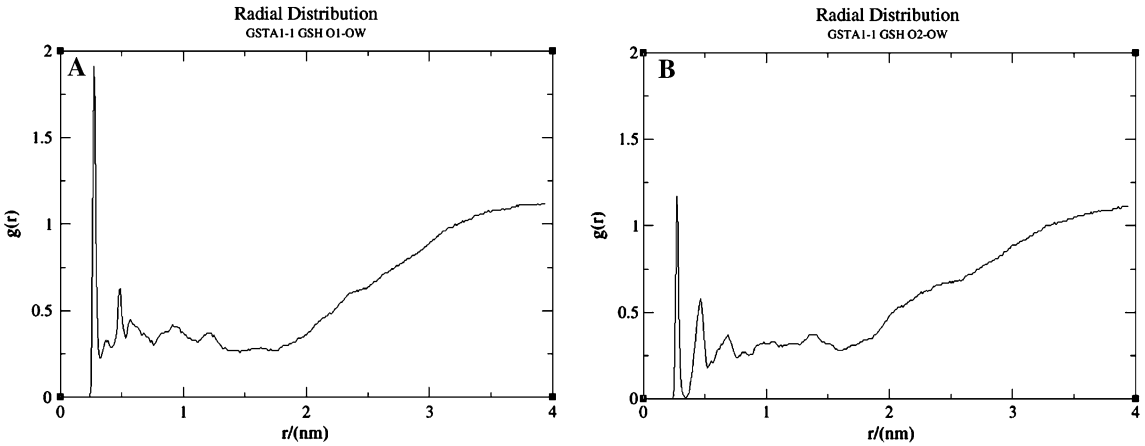

Fig. 4 Subunits 1 and 2 average GSTA1-1 radial distribution function of each GSH COO oxygen atoms separately. **a** O1–OW. Coordination sphere—two water molecules; **b** O2–OW. First coordination sphere—one water molecule, second coordination sphere—four water molecules and third coordination sphere—eight water molecules

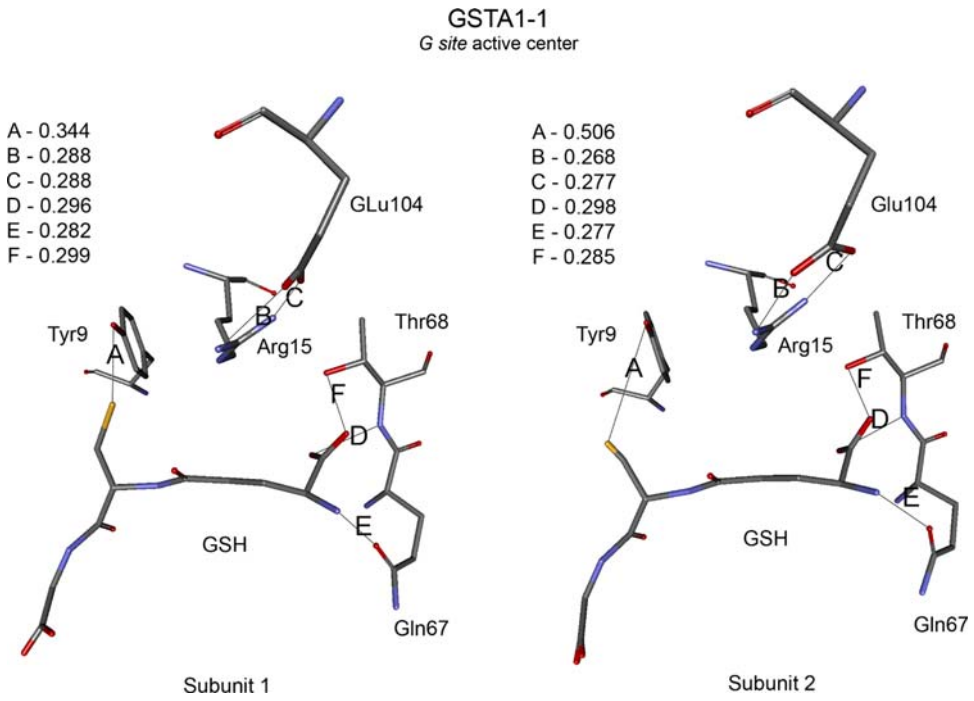

Fig. 5 GSTA1-1 *G-site* pocket average structures for both the subunits 1 and 2. Relevant distances (nm) are shown

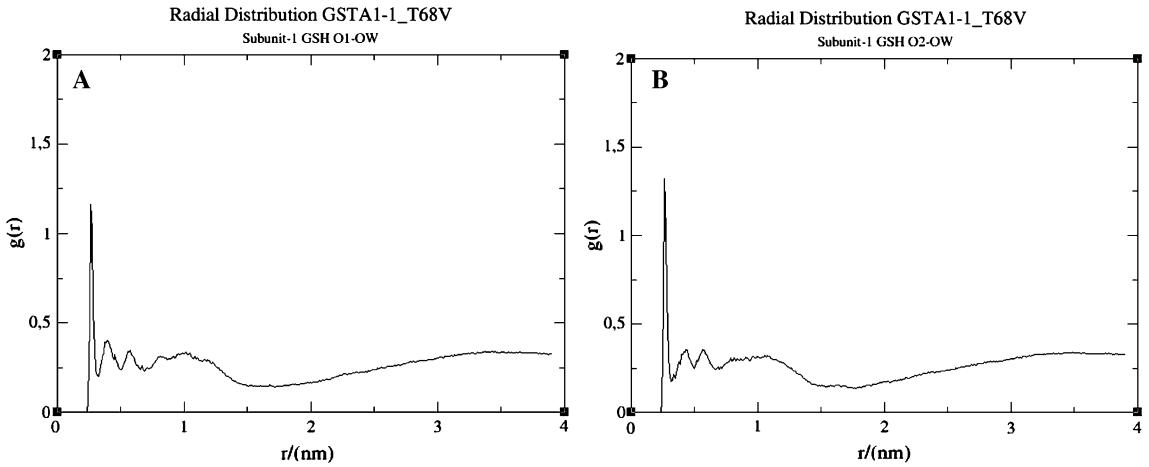

Fig. 6 Subunit 1 GSTA1-1_T68V radial distribution function of each GSH COO oxygen atoms separately. **a** O1–OW. Coordination sphere—1.3 water molecules; **b** O2–OW. First coordination sphere—1.3 water molecules

3.3.2 GSTA1-1_T68E

In this mutant, the water around the GSH thiol group is organized in a way similar to that in the wild-type enzyme (Fig. 3). The subunits average S–OW RDF peak starts at 0.285 nm, has a maximum at 0.350 nm and goes to zero at 0.478 nm with a total of five water molecules.

The water arrangement around the GSH glutamyl alpha carboxylate of GSTA1-1_T68E (Fig. 8) changes very significantly when compared to the wild-type enzyme (Fig. 4).

In the O–OW RDF plots, only one defined water coordination sphere is observed. Contrary to what happens with the wild-type enzyme, the water molecules are roughly equally distributed around the two oxygen atoms of the alpha carboxylic group.

The *G-site* MD average structures presented some differences between the two subunits (Figs. 9, 10).

The GSH thiol group is hydrogen bonded to Tyr9 sidechain in both the subunits (Figs. 9a, 10a). The hydrogen bond between the GSH glutamyl alpha carboxylate and the residue 68 mainchain is maintained similar to what happens in GSTA1-1_T68V (Figs. 9d, 10d).

The new position of the Gln67 side chain precludes the formation of a hydrogen bond with the GSH glutamyl alpha amino group (Figs. 9e, 10e). Analyses of GSTA1-1_T68E

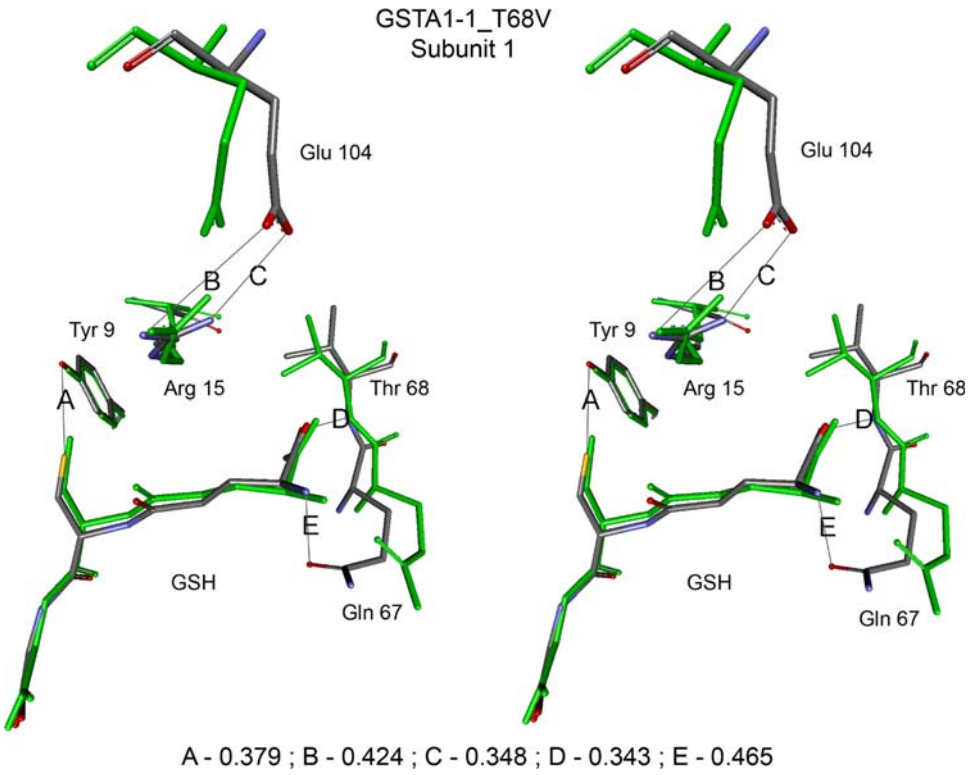

Fig. 7 Stereo view of GSTA1-1_T68V Subunit 1 *G-site* average structure superimposed with GSTA1-1 Subunit 1 *G-site* average structure (*green*). Relevant distances (nm) are shown

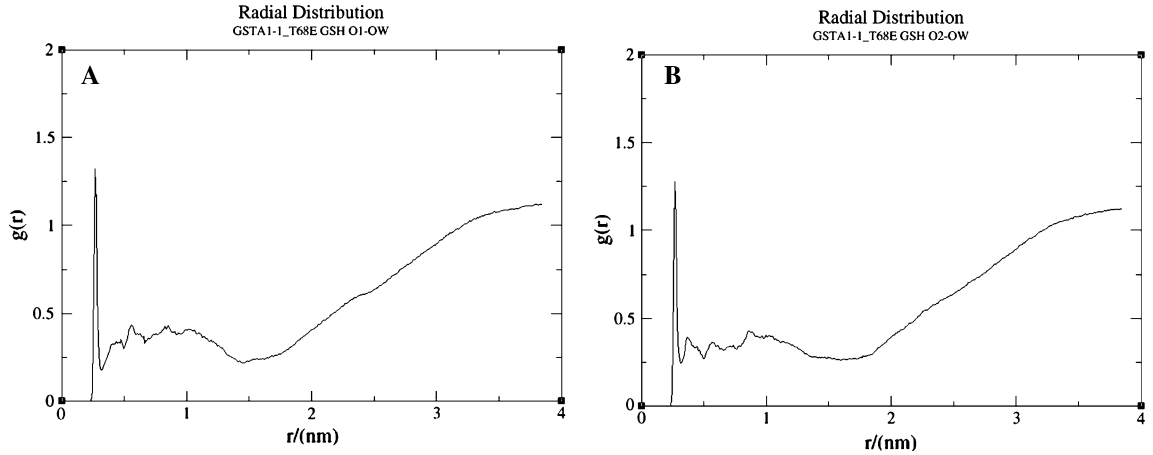

Fig. 8 Subunits 1 and 2 average GSTA1-1_T68E radial distribution function of each GSH COO oxygen atoms separately. **a** O1–OW. Coordination sphere—1.3 water molecules; **b** O2–OW. Coordination sphere—1.3 water molecules

and GSTA1-1_T68V (Fig. 7) allowed us to conclude that the new position of residue 67 should have a fundamental role in the changes observed for the water organization around the GSH glutamyl alpha carboxylate.

As mentioned beforehand, the initial structure of GSTA1-1_T68E had a different Glu68 rotamer for each subunit. In subunit 1, the Glu68 side chain is turned to the GSH glutamate carboxylic group, and in subunit 2, it occupies the opposite direction as seen in the recent GSTA1-1_T68E crystallographic structure, in which a Cl^- ion is taking the place of the alpha carboxylic group of GSH glutamate [13]. MD analyses have shown that after 150 ps, Glu68 in subunit 1 moves away from GSH ending in a similar position as that of Glu68 in subunit 2. On the other hand, the charged Glu68 in both the subunits seems to displace Glu104, establishing a strong ion–ion interaction with Arg15 (Figs. 9f, 10f), a strictly conserved residue in class alpha GSTs. Therefore, all these strong steric and charge repulsive effects caused by the different positioning of Glu68 lead to considerable changes in the GSH pocket, which are consistent with the increase in the K_M^{GSH} of ~18-fold [2] described for this mutant.

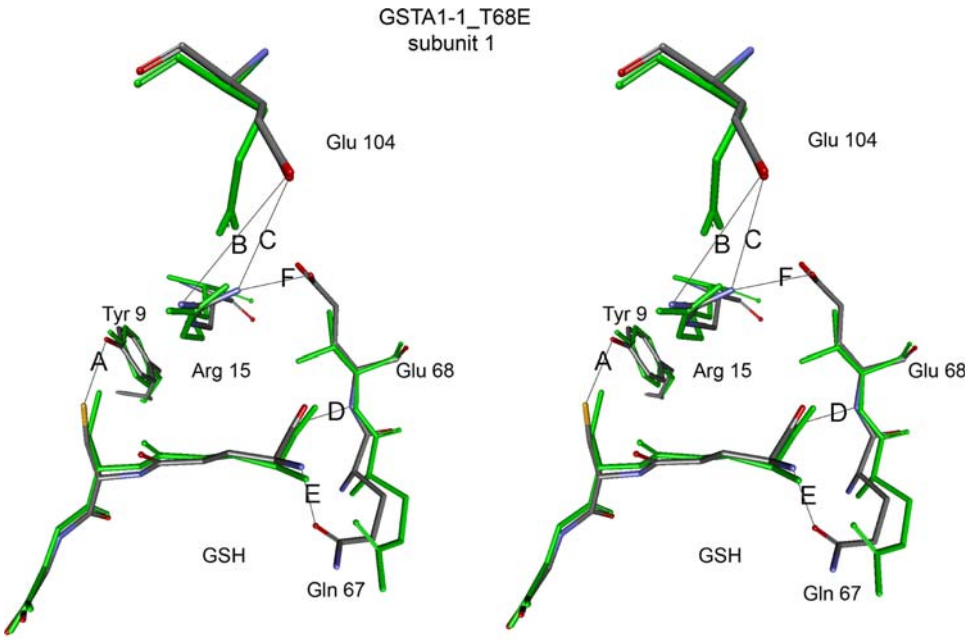

Fig. 9 Stereo view of GSTA1-1_T68E subunit 1 *G-site* average structure superimposed with GSTA1-1 Subunit 1 *G-site* average structure. Relevant distances (nm) are shown

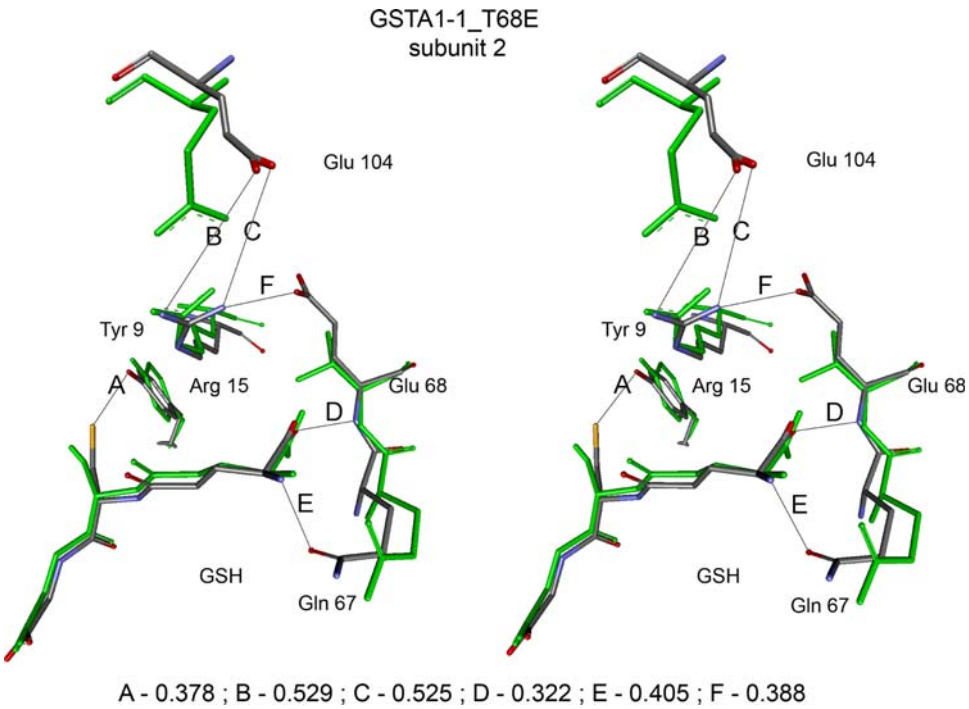

Fig. 10 Stereo view of GSTA1-1_T68E Subunit 2 *G-site* average structure superimposed with GSTA1-1 Subunit 2 *G-site* average structure. Relevant distances (nm) are shown

3.4 GSTA1-1_dGSH

Looking at the subunits average S–OW RDF plot of GSTA1-1_dGSH (Fig. 11), we can see that the water is badly distributed around the dGSH thiol group. The peak corresponds to two water molecules only.

Therefore, without the alpha carboxylic group, the substrate seems to loose most of its water coordination sphere previously observed in solution and in the wild-type enzyme.

Comparing the average structures of GSTA1-1dGSH and GSTA1-1 (Figs. 12, 13), we realized that with the loss of the carboxylate group, the substrate also loses important interactions in the *G-site* pocket in both the subunits, namely the hydrogen bond between Gln67 and the substrate amino group, since Gln67 sidechain adopts a

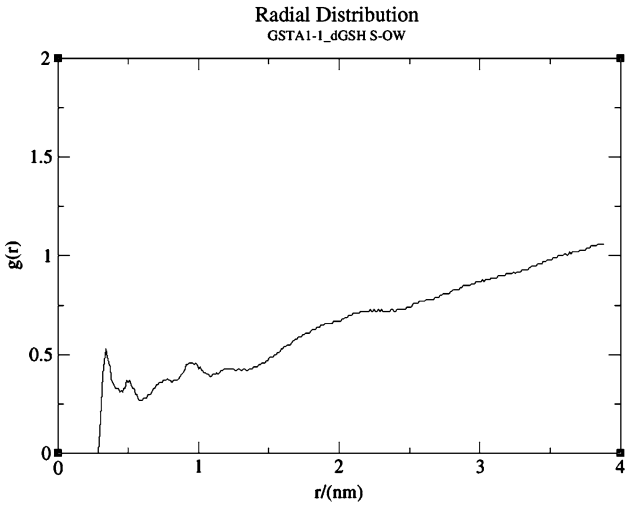

Fig. 11 Subunits 1 and 2 average GSTA1-1_dGSH dGSH S–OW radial distribution function. Coordination sphere—two water molecules

different conformation (Figs. 12d, 13d). This lower affinity with the *G-site* pocket leads to a somewhat different spatial arrangement of the substrate, and is consistent with a K_M^{dGSH} 100–fold higher than the K_M^{GSH} [2].

3.5 GSTA1-1_dGSH mutants

3.5.1 GSTA1-1_T68D_dGSH

For GSTA1-1_T68D_dGSH, the water arrangement around the thiol group, lost in GSTA1-1_dGSH (Fig. 11), is now similar to the one found for the wild-type enzyme (Fig. 3). The average S–OW RDF peak of the subunits starts at 0.285 nm, has a maximum at 0.345 nm and goes to zero at 0.434 nm with a total of five water molecules.

Analyses of the average O–OW RDF peak of the subunits for each of the Asp68 side chain carboxylic group oxygens revealed that the water molecules are equally distributed around both, contrary to what happens for the wild-type enzyme.

Average structures of GSTA1-1_T68D_dGSH have shown that similar to that in the other mutants, Gln67 adopted a different conformation that precludes the formation of a hydrogen bond with the dGSH glutamyl alpha amino group. It is also observed that substrate dGSH adopts a bent conformation not seen in GSTA1-1_dGSH. In both the subunits, Asp68 is not facing the dGSH amino group.

3.5.2 GSTA1-1_T68E_dGSH

For GSTA1-1_T68E_dGSH, the S–OW RDF peak, just as in the previous case, is identical to the one observed for the wild-type enzyme (Fig. 3); therefore, it points to a recovery of the water arrangement around the substrate thiol lost in GSTA1-1_dGSH complex (Fig. 11). The peak starts at 0.285 nm, has a maximum at 0.345 nm and goes to zero at 0.445 nm with a total of six water molecules.

We have started the simulation from a structure with different Glu68 rotamers in each subunit. In subunit 1, Glu68 was turned to dGSH, while in subunit 2 it was facing

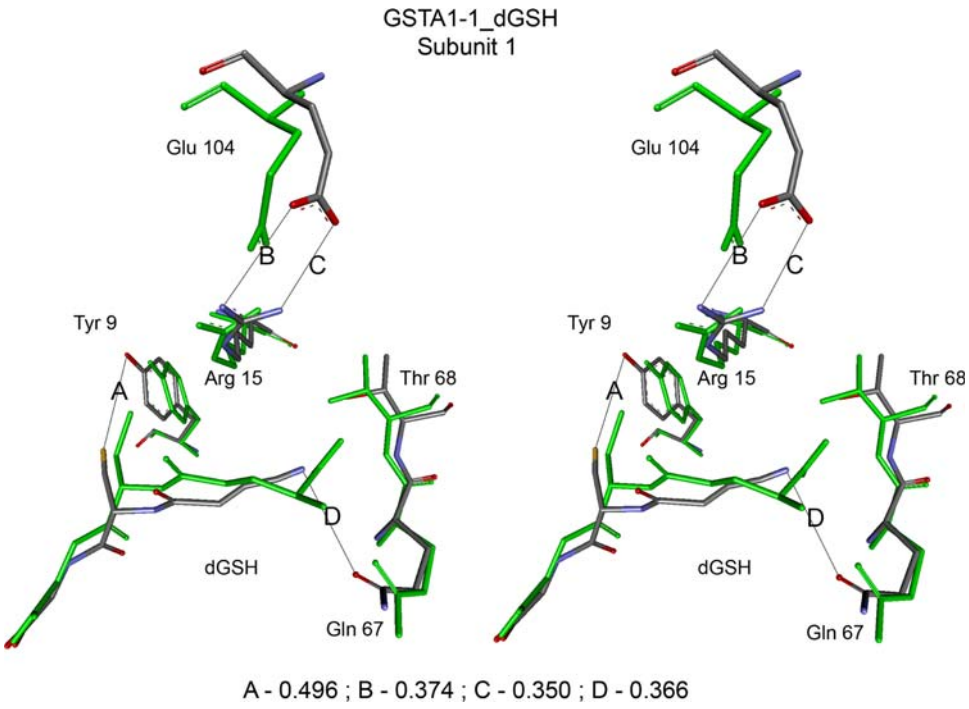

Fig. 12 Stereo view of GSTA1-1_dGSH subunit 1 *G-site* average structure superimposed with GSTA1-1 subunit 1 *G-site* average structure. Relevant distances (nm) are shown

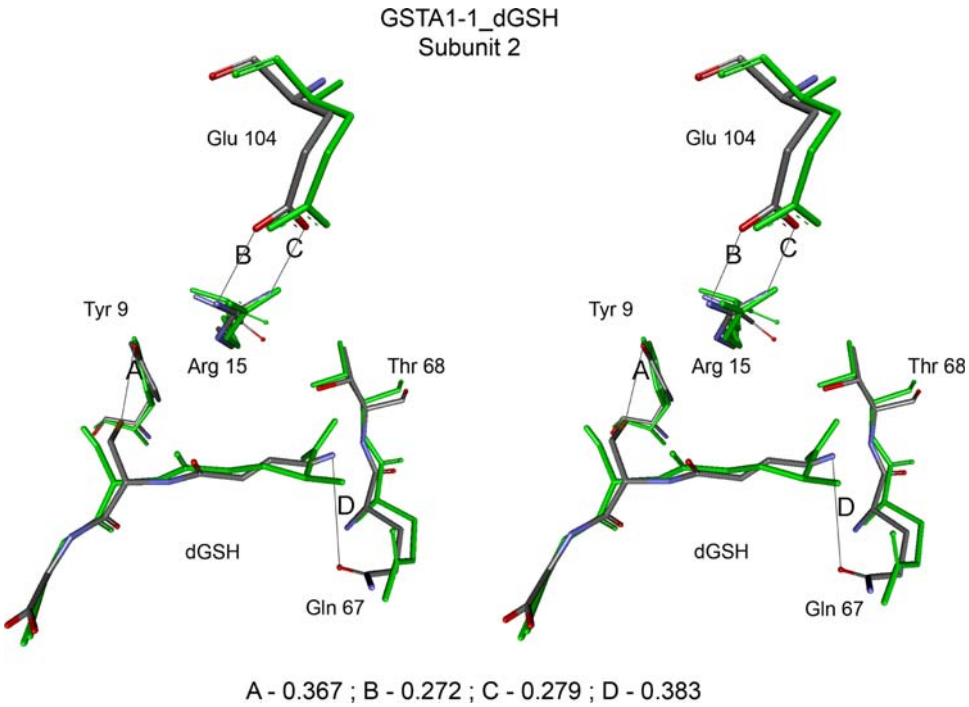

Fig. 13 Stereo view of GSTA1-1_dGSH subunit 2 *G-site* average structure superimposed with GSTA1-1 subunit 2 *G-site* average structure. Relevant distances (nm) are shown

the opposite direction as seen in the recent GSTA1-1_T68E crystallographic structure, in which a Cl^- ion is taking the place of the alpha carboxylic group of GSH glutamate [13]. During the simulation, there were not any significant changes in the rotamers of residue 68. The analysis of the MD trajectory demonstrated that the water arrangement around the Glu68 carboxylic group of subunit 1 (Fig. 14a) is comparable to the one obtained for the GSH glutamyl alpha carboxylate in the wild-type enzyme (Fig. 4). Glu68 O–OW RDF plots of subunit 1 point to an asymmetric water organization around the oxygen atoms. A very well-defined first coordination sphere corresponding to a single water molecule was observed around the oxygen more close to the thiol group (Fig. 14a, c), as in the case of the wild-type enzyme complexed with GSH (Fig. 4b). It was also noticed that in subunit 1, dGSH changes to a different position with the substrate amino group oriented towards the Glu68 side chain carboxylic group (Fig. 15f). In addition, in this subunit, Arg15 seems to make a salt bridge with Glu68 sidechain (Fig. 15e). In both the subunits, residue Gln67, similar to that in other mutants, seems to be too far away from the substrate amino group to interact with it (Figs. 15d, 16d).

Since the analysis of this mutant could allow for fundamental insights on the relation between the *G-site* water molecules and catalysis, to further elucidate which Glu68 rotamer nature favours, we decided to extend the MD simulation to 20 ns. The subsequent analysis has shown that in subunit 2, Glu68 maintained its initial position, hydrogen bonded with Arg15, throughout the 20 ns simulation. On the other hand, the substrate moved away from the *G-site* after10 ns. In subunit 1, the Glu68 side chain keeps its initial rotamer during almost the whole simulation (except in between 9.8 and 10.6 ns) and dGSH remains in the *G-site* for the entire 20 ns simulation. It was also observed that for this subunit, the 20 ns MD simulation RDF plots are identical to the 3 ns MD simulation plots shown above. Therefore, Glu68 with the side chain facing the *G-site* pocket seems fundamental for a correct fit between dGSH and the *G-site* pocket and, as mentioned above, is surrounded by a water arrangement that resembles the one observed for the GSH glutamyl alpha carboxylate in the wild-type enzyme.

4 Conclusions

The water coordination spheres found around the GSH thiol and the glutamate alpha carboxylate in solution do not change much when the substrate GSH binds to the *G-site* of GSTA1-1, even though they present a somewhat lower intensity. The number and position of the peaks are similar, but the number of coordinated water molecules is smaller, as expected. On the other hand, if we analyze each one of the alpha carboxylic oxygen atoms separately, we realize that when GSH is complexed with GSTA1-1, the water distribution is not symmetrical, in opposition to what happens with GSH in solution, the oxygen atom being

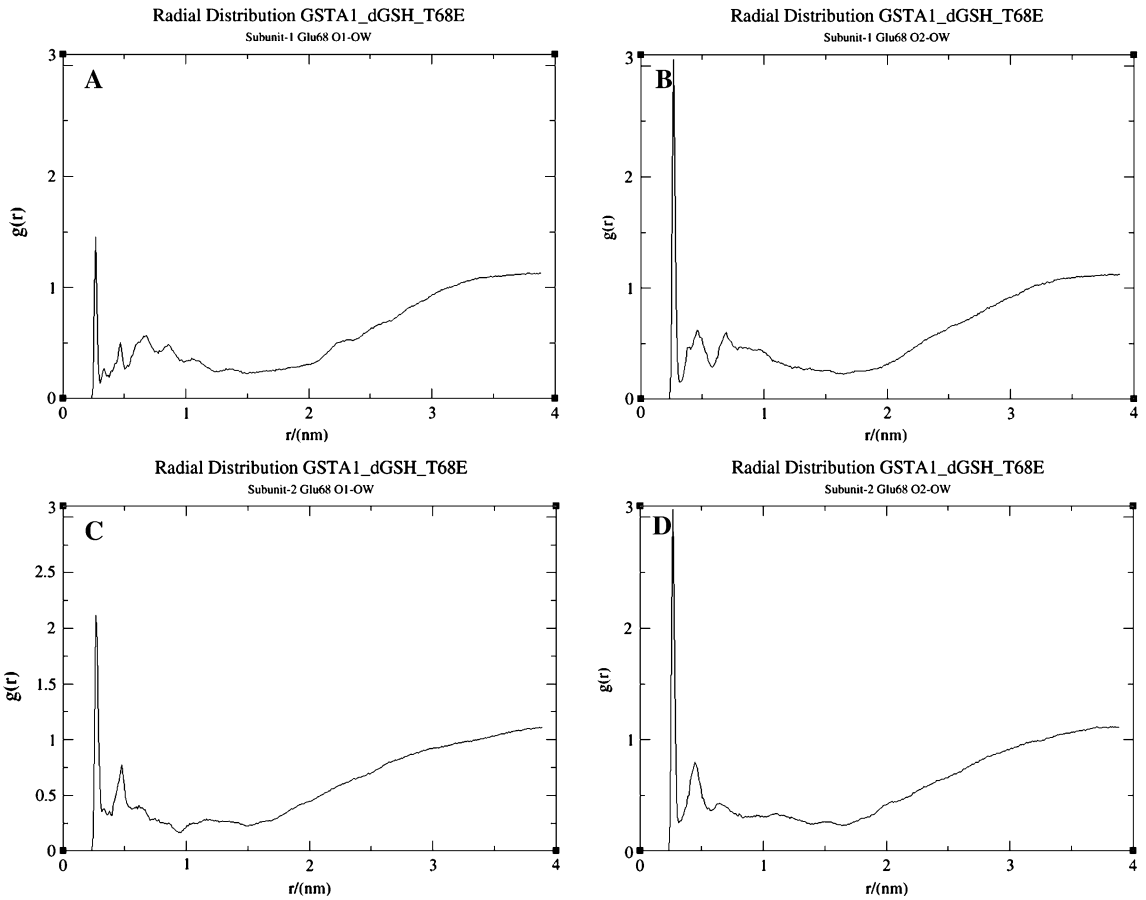

Fig. 14 GSTA1-1_T68E_dGSH radial distribution function of each dGSH COO oxygen atoms separately. **a** Subunit 1 O1–OW. Coordination sphere—1 water molecule; **b** subunit 1 O2–OW. First coordination sphere—2.4 water molecules, second coordination sphere 8.6 water molecules. **c** Subunit 2 O1–OW. First coordination sphere—two water molecules, second coordination sphere—6.6 water molecules; **d** subunit 2 O2–OW. First coordination sphere—2.5 water molecules, second coordination sphere—7.4 water molecules

closer to the thiol group privileged by a better defined water organization. In fact, around this oxygen, an extremely defined O–OW RDF peak points to a first coordination sphere composed of a single water molecule, followed by the other two coordination spheres composed of 4 and 8 water molecules, respectively.

Changes in catalysis observed in the mutant enzymes are accompanied by changes in the water arrangement around the GSH thiol and glutamate alpha carboxylate groups, emphasizing the importance of water molecules as promoters of GSH activation.

Analyses of the mutant enzymes complexed with GSH showed that the hydrogen bond between Gln67 side chain and the GSH alpha amino group is fundamental for a correct fit between the substrate and the *G-site* pocket, as well as for maintaining the water arrangement seen around the catalytic relevant GSH alpha carboxylic group of the wild-type enzyme. As was mentioned beforehand, the loss of the GSH alpha carboxylic group leads to a 15000 times catalytic activity drop and a rise in the p*K*a of thiol to values of a non-enzymatic reaction (6.7–9.2 pH units). Our studies show that this change in catalysis is followed by a major decrease in the water coordination sphere around the GSH thiol group. In GSTA1-1_T68D_dGSH and to a higher extent in GSTA1-1_T68E_dGSH, the catalytic activity is partially restored. We demonstrated that these mutations trigger a recovery of the water organization around the dGSH thiol group, since the S–OW RDF plots are similar to those found in the wild-type enzyme. The water organization around the GSH glutamate alpha carboxylic group of the wild-type enzyme was somewhat reproduced by the Glu68 carboxylic group of GSTA1-1_dGSH_T68E that faced the dGSH amino group. As in the wild-type enzyme, an asymmetric water arrangement was observed around the oxygens and a very well defined first coordination sphere, which corresponds to a single water molecule around the oxygen closer to the thiol group. Our studies also suggest that the Glu68 side chain should

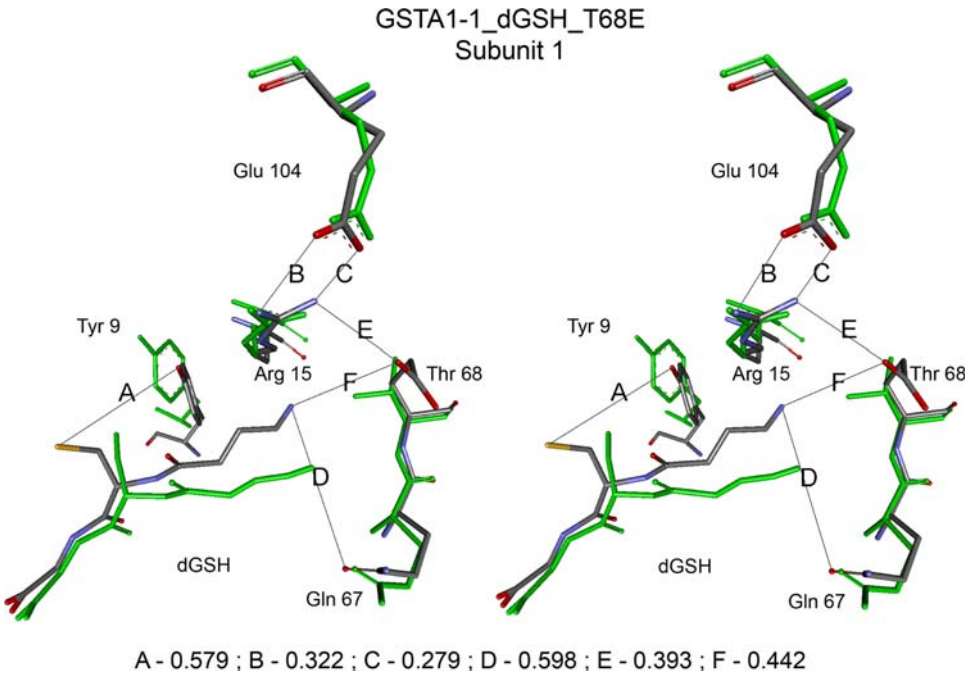

Fig. 15 GSTA1-1_dGSH_T68E Subunit 1 *G-site* average structure superimposed with GSTA1-1 subunit 1 *G-site* average structure. Relevant distances (nm) are shown

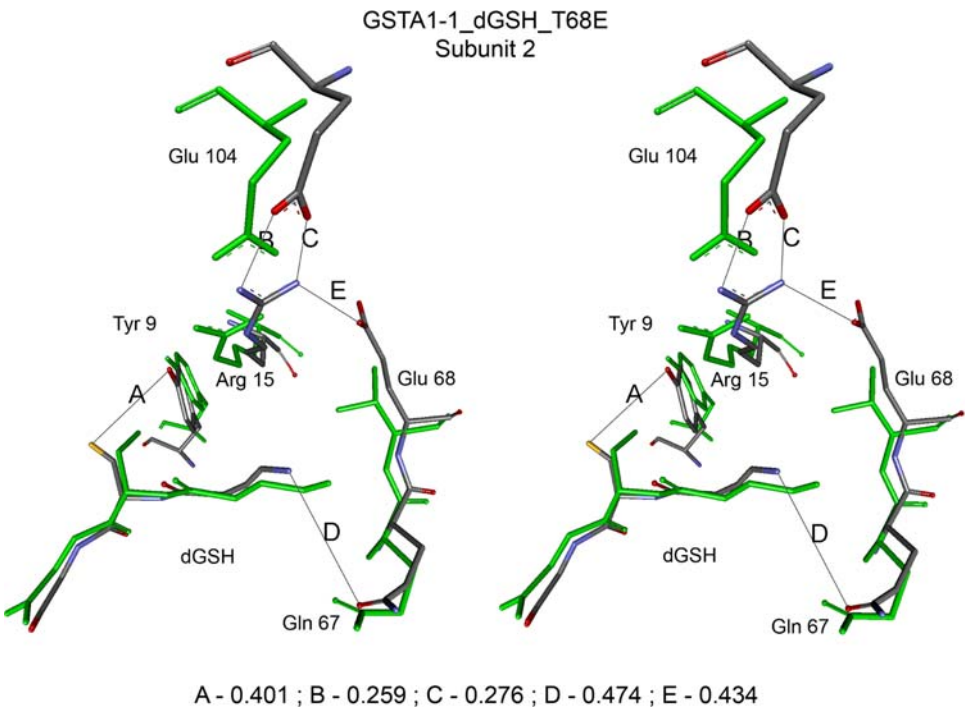

Fig. 16 GSTA1-1_dGSH_T68E Subunit 2 *G-site* average structure superimposed with GSTA1-1 subunit 2 *G-site* average structure. Relevant distances (nm) are shown

be turned to the substrate dGSH for its stable fit within the *G-site* pocket.

Therefore, it seems reasonable to think that the Glu68 carboxylic group oriented towards dGSH should be able to catalytically replace the GSH glutamate alpha carboxylic group.

5 Final remarks

Water molecules around the GSH thiol and glutamate alpha carboxylate groups confer a unique ambience that seems to determine the catalytic efficiency.

This is in agreement with the GSH activation mechanism in which a water molecule, acting as a bridge, is able to assist the transfer of the proton from the GSH thiol group to the GSH glutamyl alpha carboxylate, following an initial GSH conformational rearrangement. Such mechanism has been shown to be in agreement with the enzyme kinetics [24].

References

1. Armstrong RN (1991) Chem Res Toxicol 4:131–140. doi:10.1021/tx00020a001
2. Gustafsson A, Pettersson PL, Grehn L, Jemth P, Mannervik B (2001) Biochemistry 40:15835–15845. doi:10.1021/bi010429i
3. Sinning I, Kleywegt GJ, Cowan SW, Reinemer P, Dirr HW, Huber R, Gilliland GL, Armstrong RN, Ji X, Board PG (1993) J Mol Biol 232:192–212. doi:10.1006/jmbi.1993.1376
4. Dirr H, Reinemer P, Huber R (1994) Eur J Biochem 220:645–661. doi:10.1111/j.1432-1033.1994.tb18666.x
5. Gustafsson A, Etahadieh M, Jemth P, Mannervik B (1999) Biochemistry 38:16268–16275. doi:10.1021/bi991482y
6. Allardyce CS, McDonagh PD, Lian LY, Wolf CR, Roberts GC (1999) Biochem J 343(Pt 3):525–531. doi:10.1042/0264-6021:3430525
7. Widersten M, Bjornestedt R, Mannervik B (1996) Biochemistry 35:7731–7742. doi:10.1021/bi9601619
8. Nieslanik BS, Dabrowski MJ, Lyon RP, Atkins WM (1999) Biochemistry 38:6971–6980. doi:10.1021/bi9829130
9. Oakley AJ, Lo Bello M, Battistoni A, Ricci G, Rossjohn J, Villar HO, Parker MW (1997) J Mol Biol 274:84–100. doi:10.1006/jmbi.1997.1364
10. Cameron AD, Sinning I, L'Hermite G, Olin B, Board PG, Mannervik B, Jones TA (1995) Structure 3:717–727. doi:10.1016/S0969-2126(01)00206-4
11. Stenberg G, Board PG, Mannervik B (1991) FEBS Lett 293:153–155. doi:10.1016/0014-5793(91)81174-7
12. Bjornestedt R, Stenberg G, Widersten M, Board PG, Sinning I, Jones TA, Mannervik B (1995) J Mol Biol 247:765–773
13. Grahn E, Novotny M, Jakobsson E, Gustafsson A, Grehn L, Olin B, Madsen D, Wahlberg M, Mannervik B, Kleywegt GJ (2006) Acta Crystallogr D Biol Crystallogr 62:197–207. doi:10.1107/S0907444905039296
14. Mannervik B, Board PG, Hayes JD, Listowsky I, Pearson WR (2005) Methods Enzymol 401:1–8. doi:10.1016/S0076-6879(05)01001-3
15. Caccuri AM, Antonini G, Board PG, Parker MW, Nicotra M, Lo Bello M, Federici G, Ricci G (1999) Biochem J 344(Pt 2):419–425. doi:10.1042/0264-6021:3440419
16. Bateman A, Coin L, Durbin R, Finn RD, Hollich V, Griffiths-Jones S, Khanna A, Marshall M, Moxon S, Sonnhammer EL, Studholme DJ, Yeats C, Eddy SR (2004) Nucleic Acids Res 32:D138–D141. doi:10.1093/nar/gkh121
17. Dourado DF, Fernandes PA, Ramos MJ (2008) Curr Protein Pept Sci 9:325–337. doi:10.2174/138920308785132677
18. Karshikoff A, Reinemer P, Huber R, Ladenstein R (1993) Eur J Biochem 215:663–670. doi:10.1111/j.1432-1033.1993.tb18077.x
19. Adang AE, Brussee J, van der Gen A, Mulder GJ (1990) Biochem J 269:47–54
20. Adang AE, Brussee J, Meyer DJ, Coles B, Ketterer B, van der Gen A, Mulder GJ (1988) Biochem J 255:721–724
21. Adang AE, Meyer DJ, Brussee J, Van der Gen A, Ketterer B, Mulder GJ (1989) Biochem J 264:759–764
22. Parraga A, Garcia-Saez I, Walsh SB, Mantle TJ, Coll M (1998) Biochem J 333(Pt 3):811–816
23. Caccuri AM, Lo Bello M, Nuccetelli M, Nicotra M, Rossi P, Antonini G, Federici G, Ricci G (1998) Biochemistry 37:3028–3034. doi:10.1021/bi971903g
24. Dourado DF, Fernandes PA, Mannervik B, Ramos MJ (2008) Chemistry (Easton) 14:9591–9598
25. Berman HM, Battistuz T, Bhat TN, Bluhm WF, Bourne PE, Burkhardt K, Feng Z, Gilliland GL, Iype L, Jain S, Fagan P, Marvin J, Padilla D, Ravichandran V, Schneider B, Thanki N, Weissig H, Westbrook JD, Zardecki C (2002) Acta Crystallogr D Biol Crystallogr 58:899–907. doi:10.1107/S0907444902003451
26. Guex N, Peitsch MC (1997) Electrophoresis 18:2714–2723. doi:10.1002/elps.1150181505
27. Dennington II R, Keith T, Millam J, Eppinnentt K, Hovell WL, Gilliland R (2003) GaussView, Version 3.0. Semichem, Inc., Shawnee Mission, KS
28. Cornell WD, Cieplak P, Bayly CI, Gould IR, Merz KM Jr, Ferguson DM, Spellmeyer DC, Fox T, Caldwell JW, Kollman PA (1995) J Chem Soc 117:5179–5197. doi:10.1021/ja00124a002
29. Wang J, Wolf RM, Caldwell JW, Kollman PA, Case DA (2004) J Comput Chem 25:1157–1174. doi:10.1002/jcc.20035
30. Lindahl E, Hess B, van der Spoel D (2001) J Mol Model 7:306–317
31. Sorin EJ, Pande VS (2005) Biophys J 88:2472–2493. doi:10.1529/biophysj.104.051938
32. Berendsen H, Postma JPM, van Gunsteren WF (1981) Intermolecular forces. D. Reidel Publishing Company, Dordrecht, pp 331–342.
33. Berendsen H, Postma JPM, van Gunsteren WF, DiNola A, Haak JR (1984) J Chem Phys 81:3584–3590. doi:10.1063/1.448118
34. Essmann U, Perera L, Berkowitz ML, Darden T, Lee H, Pedersen LG (1995) J Chem Phys 103:8577–8593. doi:10.1063/1.470117
35. Hess B, Bekker H, Berendsen H, Fraaije J (1997) J Comput Chem 18:1463–1472. doi:10.1002/(SICI)1096-987X(199709)18:12<1463::AID-JCC4>3.0.CO;2-H